Journal of Alloys and Compounds 936 (2023) 168349

Contents lists available at ScienceDirect

Journal of Alloys and Compounds

journal homepage: www.elsevier.com/locate/jalcom

Research Article

Loading uniformly distributed CuRu alloys on carbon nanotubes via flash Joule heating for high-performance electrocatalytic water splitting

Wenjie Wei [a,1], Ping Li [a,1], Fenghong Lu [a], Kaicai Fan [b], Bin Li [b], Yanze Wei [c,*], Lingbo Zong [a,*], Lei Wang [a]

[a] College of Chemistry and Molecular Engineering, Qingdao University of Science and Technology, Qingdao 266042, China
[b] College of Materials Science and Engineering, Qingdao University of Science and Technology, Qingdao 266042, China
[c] Key Laboratory of Colloid and Interface Chemistry, Ministry of Education, School of Chemistry and Chemical Engineering, Shandong University, Jinan 250100, China

ARTICLE INFO

Article history:
Received 7 October 2022
Received in revised form 21 November 2022
Accepted 2 December 2022
Available online 5 December 2022

Keywords:
Ultrasmall size
Alloy nanoparticle
Flash Joule heating
Water splitting

ABSTRACT

Constructing highly efficient and stable electrocatalysts is the key to reducing the overall energy input for electrocatalytic water splitting, which ensures the reduced cost of environmentally friendly hydrogen resources with high energy density. Assisted by ultrafast pyrolysis with a flash Joule heating technique, CuRu ultrasmall alloy nanoparticles are uniformly coated on carbon nanotubes (CNTs) with tannic acid (TA) to chelate metal ions. During the pyrolysis procedure, the self-assembled TA molecules not only offer a cross-linked porous polyphenol framework but also provide more interactions to link the alloy nanoparticles and CNT substrates, forming highly conductive electrocatalysts with uniformly dispersed ultrasmall alloy metallic nanoparticles (~ 4.3 nm in diameter) on the surface of porous CNTs (CuRu-CNTs). In particular, CuRu-CNTs with Cu-Ru alloy nanoparticles achieve the highest electrochemical activity, exhibiting tiny HER and OER overpotential of 39 mV and 330 mV at 10 mA cm^{-2} in 1.0 M KOH medium. The unique bifunctional feature of CuRu-CNTs allows good overall water splitting activity (10 mA cm^{-2} for 12 h), which is comparable with the best noble metal-based benchmark. This contribution provides a general energy saving pyrolysis method for the preparation of highly efficient, cost-effective and chemically stable electrocatalysts for water splitting.

1. Introduction

The rapid growth in global energy consumption, along with rising environmental concerns about excess carbon emissions, has prompted the quest for renewable and clean energy. Among various strategies, electrochemical water splitting powered by renewables is a promising technology for large-scale green hydrogen generation [1–4]. Although the development of electrochemical water splitting has advanced in recent decades, practical applications still pose serious hurdles arising from the high energy input and catalyst cost [5,6]. Note that the electrocatalytic water splitting process includes the hydrogen evolution reaction (HER) at the cathode ($2H^+ + 2e^- \rightarrow H_2$) and the oxygen evolution reaction (OER) at the anode ($H_2O \rightarrow 1/2O_2 + 2H^+ + 2e^-$) [7]. The core challenge in advancing the technology of electrochemical water splitting to commercial viability is the sluggish reaction kinetics and complex electron transfer process [8,9]. So far, Pt and IrO_2 are considered as the most efficient HER and OER electrocatalysts in acid and basic media, respectively, but the noble metal electrocatalysts with bifunctional capacity for deriving HER and OER in the same electrolyte are scarcity [10,11]. Specially, the global reserve rare of Pt and Ir greatly hampers their scalable applications. Therefore, the development of cheaper alternatives to Pt and Ir towards high HER and OER in the same electrolyte is highly desirable.

Carbides, phosphides, sulfides, and transition metal oxides have been applied extensively in catalyzing HER and OER [12–16]. However, their catalytic performance including the overpotentials and robustness can not compare with the platinum group metal catalysts. Recently, alloying noble metals with high natural abundance transition metals is considered a feasible and promising planning to expedite the HER and OER performance [17,18]. Alloying approach has many advantages, for example, reducing the catalyst cost,

* Corresponding authors.
E-mail addresses: yzwei@sdu.edu.cn (Y. Wei), lingbozong@qust.edu.cn (L. Zong).
[1] These authors contributed equally.

https://doi.org/10.1016/j.jallcom.2022.168349
0925-8388/

regulating the electronic structure, decreasing the energy barrier, optimizing the binding energy of the key reaction intermediates, and boosting catalytic activity [19–21]. Ru, only ~ 1/3 the cost of Pt, with similar hydrogen binding energy to Pt is regarded as efficient substituent to Pt [21,22]. For the last two years, many Ru alloys catalysts with HER or OER have been developed, including binary Ru-M (M = Co [21,23–25], Ni [26–28], Cu [29], Mo [30], Au [31], Pt [32,33], Pd [34], Ir [35]), ternary PtRuIr [10], RuCoMn [36], quaternary NiIrRuAl [37] and high entropy alloy [38,39]. In spite of great progress, the exploration for the ultrafast synthesis of ultrafine Ru-based alloys supported by conductive substrates with excellent HER and OER performance in alkaline medium remains a major challenge.

Ru with excellent water dissociation kinetics in alkaline solution is adopted as encouraging electrocatalyst [40,41]. However, Ru with strong hydrogen binding strength impedes the desorption process of H. The weak Cu-H interaction between earth-abundant Cu and H atoms is regarded as the poor HER catalyst, reducing the reaction kinetics [21,42]. By alloying Ru and Cu is expected to offer exceptionally performance for both HER and OER, delivering effective strategy for water splitting [18]. In this work, we propose an ultrafast flash Joule heating pyrolysis strategy (1600 °C, 0.5 s) to fabricate CuRu alloys on carbon tubes (CuRu-CNTs) to synergistically increase the electrochemical activity and chemical stability with the aid of tannic acid (TA). Significantly, CuRu-CNTs deliver decent HER and OER catalytic activity in 1.0 M KOH solution with extremely tiny overpotentials (39 mV and 330 mV) attaining the current density of 10 mA cm^{-2}. Notably, CuRu-CNTs display outstanding robustness with no deterioration of activity after HER and OER (16 h and 10 h) testing. Moreover, the overall water splitting performance of bifunctional CuRu-CNTs electrocatalysts is superior to the noble metal-based benchmark (1.67 vs 1.72 V, at j = 10 mA cm^{-2}) at a low catalyst loading capacity of 0.255 mg cm^{-2} in 1.0 M KOH solution. This work provides an easily accessible, green and energy-saving approach for fabricating many electrocatalysts with encouraging performance.

2. Experimental section

2.1. Materials

All the chemicals were analytical grade and used without further purification. Tannic acid (TA, $C_{76}H_{52}O_{46}$) was purchased from Macklin Biochemical Co., Ltd. NaOH, KOH, and $CuCl_2{\cdot}2H_2O$ were purchased from Sinopharm Chemical Reagent Co., Ltd. $RuCl_3$ was purchased from Shanghai Aladdin Biochemical Technology Co., Ltd. Pt/C (20 wt%), Nafion solution, and RuO_2 (99.95 %) were supplied by Alfa Aesar. Carbon nanotubes (CNTs) were purchased from Nanjing XFNANO Materials Tech Co., Ltd. Carbon cloths (CCs) were purchased from Suzhou Sinero Technology Co., Ltd. Ultra-pure water (18.2 MΩ cm^{-2}) was used in this work.

2.2. Synthesis of CuRu-CNTs

Cupric chloride dihydrate ($CuCl_2{\cdot}2H_2O$, 0.10 mmol) and Ruthenium chloride ($RuCl_3$, 0.10 mmol) were dissolved in deionized water (DI Water, 10 mL) mixed with 0.05 g carbon nanotubes (CNTs) and then ultrasonicated for 1 h at room temperature. Then, 6.67 mL of tannic acid (9 mg mL^{-1}) solution and 33.3 μL of NaOH (2.0 M) solution were quickly added to the beaker and stirred for 10 min. The homogeneous solution was heated to 90 °C and kept for 8 h in a water bath. After the solution was cooled to room temperature, it was washed three times with DI water and centrifuged, and then, the samples were dried at 60 °C for 6 h. The dried samples were then rapidly sintered in a Joule furnace at 1600 °C 0.5 s^{-1} under nitrogen protection, which was labeled CuRu-CNTs.

2.3. Synthesis of Cu-CNTs and Ru-CNTs

Cu-CNTs and Ru-CNTs were fabricated according to the same procedure as CuRu-CNTs. The only difference is that solo chloride salt was added into the mixture as a metal precursor.

2.4. Material characterizations

A JEM-2100UHR at an accelerating voltage of 200 KV was used to characterize the morphologies of materials by transmission electron microscopy (TEM) and high resolution TEM (HRTEM). Field emission scanning transmission electron microscopy (FE-SEM, Sigma 500, Zeiss) was used to analyze the size and shape of the as-prepared electrocatalyst. To characterize the structure and chemical state of the samples, X-ray diffraction (XRD) patterns were obtained by a Rigaku X-ray diffractometer. X-ray photoelectron spectroscopy (XPS, K-Alpha, USA) was performed using an ESCALAB 250Xi instrument. Raman spectra were obtained by an inVia spectrometer with an excitation laser wavelength of 532 nm.

2.5. Electrochemical measurements

Electrochemical tests were carried out on an electrochemical workstation (CHI760E, Shanghai, China) based on a classical three-electrode system. The Hg/HgO electrode and a graphite rod were used as the reference electrode and the counter electrode, respectively. A glassy carbon rotating disk electrode (RDE) (diameter: 5 mm, area: 0.196 cm^2) loaded with the electrocatalyst ink was applied as the working electrode. The electrocatalyst ink (5 mg mL^{-1}) was prepared by sonicating a mixture of electrocatalysts (5 mg), H_2O (240 μL), isopropanol (720 μL) and 5 wt% Nafion (40 μL) (volume ratio = 6:18:1) until a homogeneous dispersion was obtained. Then, 10 μL of the electrocatalyst ink was dropped on the RDE electrode and dried at room temperature naturally. The HER and OER were conducted in 1.0 M KOH electrolyte with a scan rate of 5 mV s^{-1}. For the stability test, the electrocatalyst ink was deposited on carbon cloths (CCs) and then dried naturally to carry out chronopotentiometry measurements.

3. Results and discussion

3.1. Morphological and structural characterization

The synthetic strategy is illustrated in Fig. 1a, which clearly shows the flash Joule heating approach to yield CuRu-CNTs with promising potential for large-scale applications. Tannic acid (TA) with its strong affinity for metals form the tris-complex under alkaline solution and the phenolic groups of TA can significantly adsorb on CNTs, boosting the interaction between conductive substrate and the metal ions [43,44]. Subsequently, CuRu alloy nanoparticles are obtained through the ultrafast flash Joule heating method via fast heating the sample to 1600 °C in a nitrogen-filled acrylic box within 0.5 s. Scanning electron microscope (SEM) image in Fig. 1b clearly exhibits the well-preserved one-dimensional (1D) morphology of CNTs, which have an average diameter of approximately 38 nm (untreated CNTs: ~ 36 nm, Fig. S1). The transmission electron microscope (TEM) image reveals more details of CuRu-CNTs. Even at low Cu and Ru loading amounts (Fig. S2), ultrasmall CuRu alloy nanoparticles could be clearly observed in Fig. 1c. As shown in Fig. S3, Cu-CNTs and Ru-CNTs have similar morphological characteristics to CuRu-CNTs. Notably, the high-resolution TEM (HRTEM) images of Fig. 1d, e show the distinct regions of the catalyst's surface, with clear carbon layers indicating the wall of CNTs and nanoparticles with well-defined lattice fingerprint prints of 0.205 and 0.214 nm that are characteristic of the (101) and (001) planes of hcp Ru (PDF #06-0663) (Fig. 2a) [45]. This indicates the formation of ultrasmall

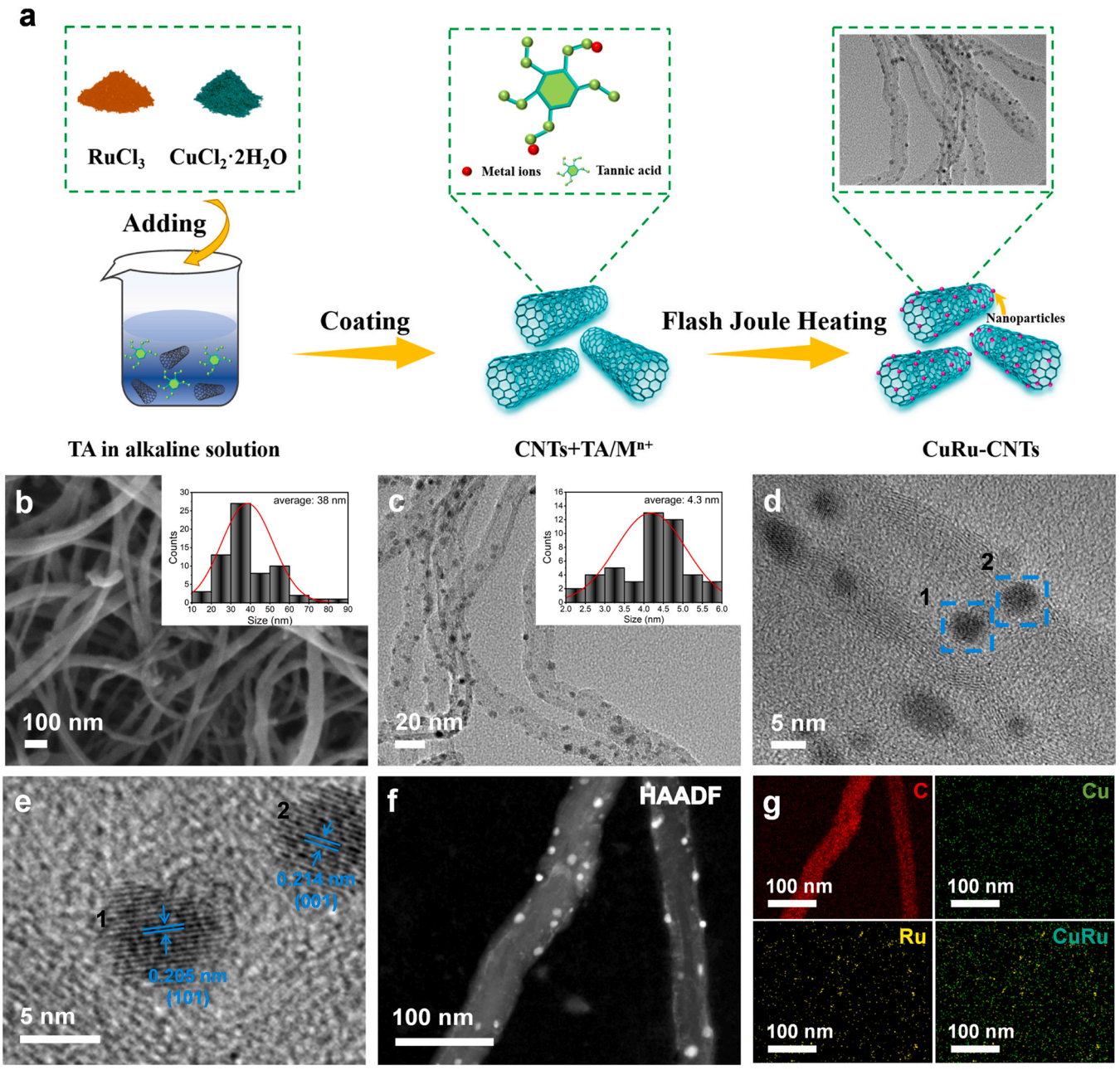

Fig. 1. (a) Schematic illustration of the synthesis route of CuRu-CNTs. (b) SEM image, and (c) TEM image with corresponding size distributions, (d) HRTEM image, (e) HRTEM image recorded from (d), (f, g) HAADF-STEM image and elemental mappings of C, Cu, Ru and CuRu of CuRu-CNTs.

metallic nanoparticles of approximately 4.3 nm uniformly dispersed on the surface of porous CNTs. Moreover, the close contact confirmed by HRTEM strongly indicates the existence of metal-support interactions within the CuRu-CNTs. As shown in the high-angle annular dark field (HAADF) STEM and energy-dispersive X-ray spectroscopy (EDX) results, almost uniformly dispersed ultrasmall particles composed of Cu and Ru elements are observed in the carbon substrate (Fig. 1f, g), testifying the successful alloying of Cu and Ru. We believe that TA molecules play important roles in the formation of spatially distributed CuRu alloy nanoparticles. The abundant phenolic groups not only provide strong surface adhesion to CNTs but also efficiently capture metal ions [46,47]. During the ultrafast heating process, TA can undergo self-polymerization to yield porous scaffolds, which would increase the collisions between reactants and the active sites [48]. As a consequence, the well-retained 1D tubular structure and uniformly embedded CuRu nanograins are confirmed on CuRu-CNTs. In comparison, Cu-CNTs and Ru-CNTs are synthesized via the same conditions without $RuCl_3$ and $CuCl_2{\cdot}2H_2O$, respectively (Fig. S4 and Fig. S5).

The crystal features of CuRu-CNTs were then evaluated. The X-ray diffraction (XRD) patterns of the as-synthesized CuRu-CNTs, Cu-CNTs, and Ru-CNTs (Fig. 2a, Fig. S6) all show two broad diffraction peaks obviously located at 26° and 44°, which could be attributed to the (002) and (101) planes of the partially graphitized carbon [49–51]. Remarkably, characteristic peaks belonging to solo Ru are detected in the XRD characterization, while the absence of characteristic peaks of metallic Cu may be due to the low doping amount of Cu (0.85 wt%, ICP-OES) (Table S1), which matches well with the above morphological observations. As shown in Fig. 2b and Fig. S7, D and G bands can be observed at 1350 and 1580 cm^{-1} in Raman measurements, which are related to disorder-related carbon (D band) and graphitic-induced sp^2-hybridized carbon (G band),

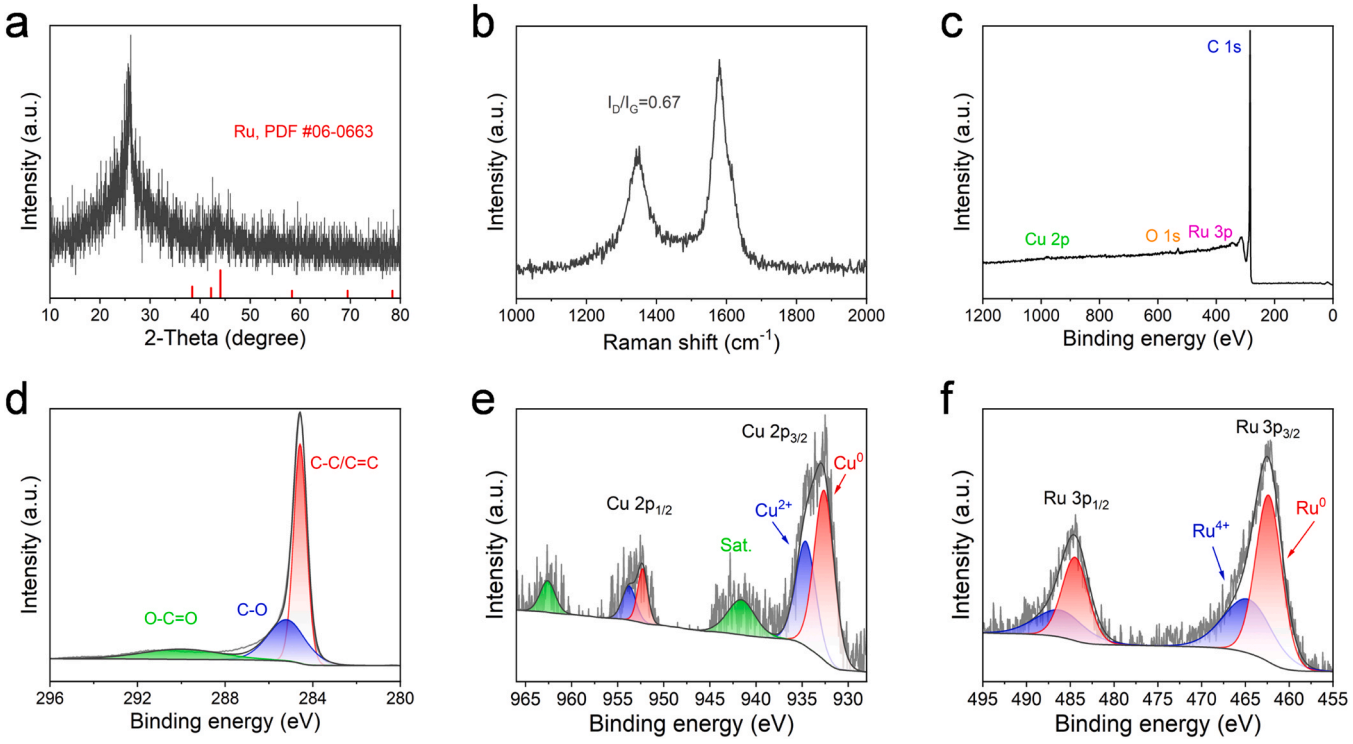

Fig. 2. (a) XRD pattern, (b) Raman spectrum, (c) XPS survey spectrum, and high-resolution XPS spectra of (d) C 1s, (e) Cu 2p, and (f) Ru 3p of CuRu-CNTs.

respectively [52,53]. The intensity ratios of I_D/I_G of CuRu-CNTs, Cu-CNTs, and Ru-CNTs are 0.67, 0.57, and 0.59, respectively, implying a high degree of graphitization in the electrocatalysts. Among them, CuRu-CNTs have the highest I_D/I_G ratio, indicating that the Cu-Ru bimetallic synergy contributes to the generation of defects and vacancies while ensuring a high degree of graphitization. The highly conductive graphite structure is necessary for continuous fast electron transfer in electrocatalytic processes, which prevents heat accumulation on the electrodes and reduces the dissipation of input energy [54,55].

According to the XPS survey spectrum of CuRu-CNTs, the atomic percentages for Cu and Ru are calculated to be 0.07 % and 0.32 %, respectively (Fig. 2c). Sensitive high-resolution XPS spectra provide more information about the electronic structures of CuRu-CNTs. Fig. 2d presents the high-resolution C 1s XPS result of CuRu-CNTs. The rather low intensity of the O-C═O and C-O peaks shows a limited content of oxygen-containing functional groups in the catalyst [44,56], which suggests that no obvious oxidation occurred to CNTs in the sample preparation procedure. According to the detection of two forms of Cu species in Fig. 2e, including Cu^0 and Cu^{2+}, the Cu^0 2p3/2 and Cu^0 2p1/2 peaks at 932.6 and 952.3 eV are from metallic Cu [57]. The Cu^{2+} 2p3/2 and Cu^{2+} 2p1/2 peaks are located at 934.6 and 953.8 eV [58]. Additionally, the Ru 3p XPS result (Fig. 2f) indicates a mixed valance state of Ru, showing the major metal Ru^0 (Ru 3p3/2 and Ru 3p1/2 are located at 462.2 eV and 484.4 eV, respectively) and Ru^{4+} ions (Ru 3p3/2 and Ru 3p1/2 are located at 464.7 eV and 486.2 eV, respectively) [18,58]. Notably, a higher ratio of Ru^{4+}/Ru^0 is beneficial to the formation of oxygen intermediates during the OER [59,60]. Specially, the abundant Ru^0 can weaken the hydrogen binding energy of the Ru site, which is beneficial to its HER activity [18,61]. The electronic structure changes of Cu and Ru during alloying were studied by comparing the high-resolution XPS spectra of CuRu-CNTs with those of Cu-CNTs and Ru-CNTs. Compared with Cu-CNTs, the Cu 2p peak of CuRu-CNTs gradually shifted to higher binding energy, while the Ru 3p peak of CuRu-CNTs is negatively shifted compared to Ru-CNTs and moves in the direction of low binding energy (Fig. S8, were marked with a dotted line.). The results suggest strong electronic interaction and electron transfer effect between the Ru and Co atoms in the Co-Ru alloy nanoparticles [21,42].

3.2. Electrocatalytic performance toward HER and OER

Next, the HER and OER activities of the synthesized CuRu-CNTs were investigated in 1 M KOH solution by a three-electrode system. The performances of the as-synthesized samples in the HER were investigated. The LSV curves of CuRu-CNTs, Cu-CNTs, Ru-CNTs, and Pt/C catalysts conducted in 1 M KOH are shown in Fig. 3a. CuRu-CNTs show a quite similar overpotential of 39 mV to Pt/C, which is much lower than those of Cu-CNTs (423 mV) and Ru-CNTs (131 mV). The Tafel slope of CuRu-CNTs suggests the merit of the porous structure within the electrocatalysts: CuRu-CNTs exhibit the lowest slope of 89 mV dec^{-1}, which is even lower than that of Pt/C (96 mV dec^{-1}) (Fig. 3b). Electrochemical impedance spectroscopy (EIS) reveals that CuRu-CNTs have a lower charge transfer resistance (≈ 15 Ω), which is beneficial for charge transport through the CuRu-CNTs cathode (Fig. 3c). CuRu-CNTs sample shows a higher Cdl value (3.4 mF cm^{-2}), which can explain the high ECSA (85 cm^2) [62,63] and high electrocatalytic activity for the HER (Fig. S9). Furthermore, the alloying of Ru and Cu with improving H_2O dissociation and optimizing H binding energy can account for boosting HER performance in alkaline medium [21,42]. Similarly, as shown in Fig. 3d, the Pt/C catalyst suffers from a quickly decreasing current density within 8 h, retaining only 13.0 % of the initial activity. In contrast, the current density of the CuRu-CNTs obtained by chronoamperometry for 16 h retains 91.0 % of its initial value, which is much higher than that of Pt/C (13.0 %) and confirms the superior durability of CuRu-CNTs without a significant loss of activity. In addition, the CuRu-CNTs exhibit excellent structural stability in alkaline electrolytes, as demonstrated by their well-maintained morphology after chronoamperometry (Fig. S10 and Fig. S11).

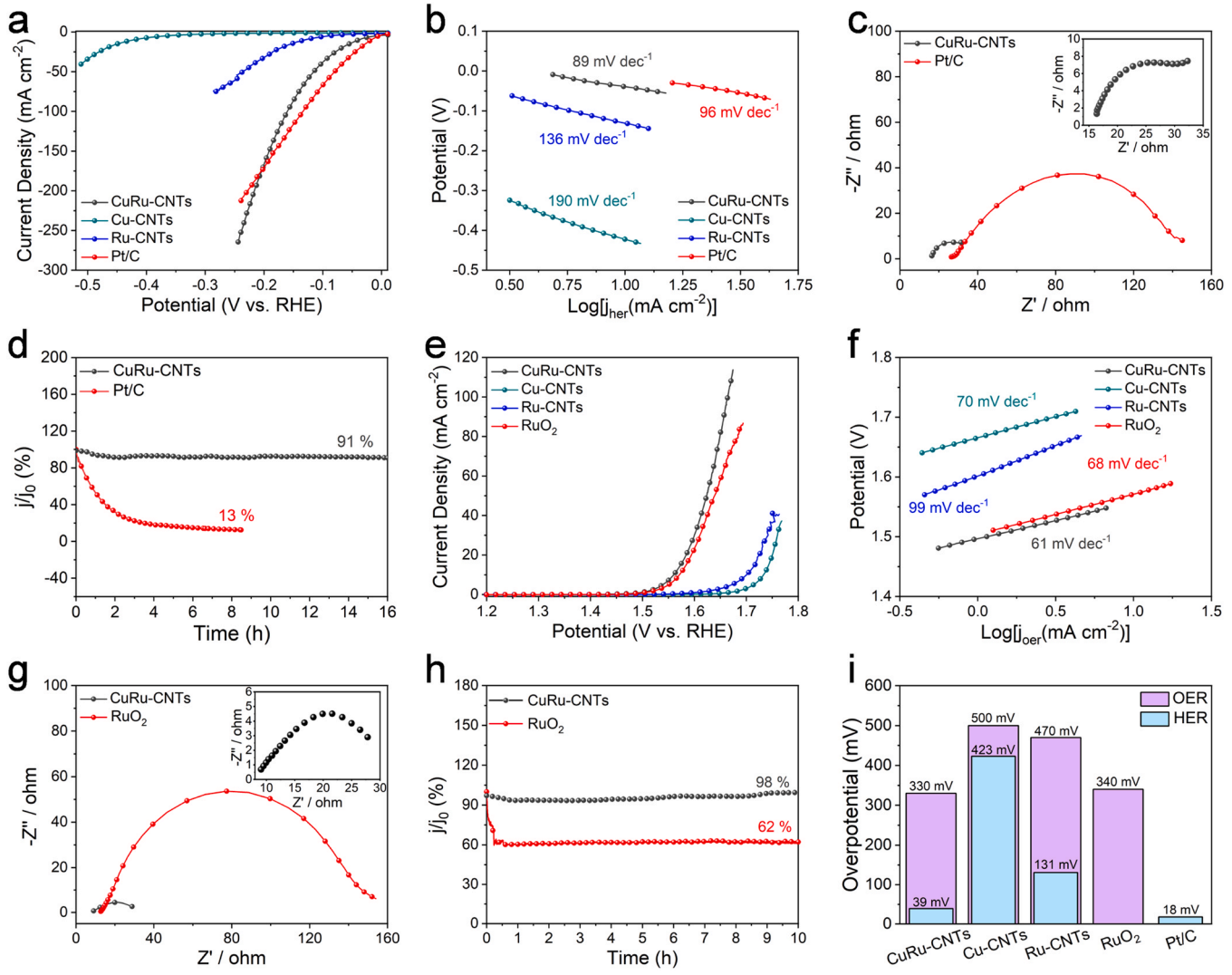

Fig. 3. (a) HER polarization curves in 1.0 M KOH, and corresponding (b) Tafel slopes, (c) Nyquist plots obtained by EIS, (d) stability test. (e) OER polarization curves in 1.0 M KOH, and the corresponding (f) Tafel slopes, (g) Nyquist plots obtained by EIS, and (h) stability test. (i) Comparison of overpotentials of different samples (at 10 mA cm^{-2}).

The performances of the as-synthesized samples in the OER were then investigated. The comparison in LSV data confirms that CuRu-CNTs have the highest OER activity with an overpotential of 330 mV to deliver 10 mA cm^{-2} current density (j_{10}), surpassing Cu-CNTs (500 mV), Ru-CNTs (470 mV), and RuO_2 (340 mV) electrocatalysts (Fig. 3e). The reaction kinetics delivered by the Tafel slopes in Fig. 3f also suggest the advantage of porous CNTs and highly accessible CuRu active sites, which demonstrates that CuRu-CNTs have the lowest Tafel slope of 61 mV dec^{-1}, in contrast to Cu-CNTs (70 mV dec^{-1}), Ru-CNTs (99 mV dec^{-1}), and RuO_2 (68 mV dec^{-1}). Furthermore, the conductivity and resistivity of the prepared catalysts were evaluated by EIS (Fig. 3g). Compared with RuO_2 catalysts, CuRu-CNTs show a lower resistance for charge transfer (Rct). The low Rct value (≈ 20 Ω) of CuRu-CNTs may be related to the high degree of graphitization and high conductivity of the carbon nanotubes and substrates, which is conducive to electron transport. To evaluate the OER durability of the highly active CuRu-CNTs, long-term chronoamperometry measurements were conducted on different samples (Fig. 3h). The activity of CuRu-CNTs remained at 98.0 % after a 10 h test, exhibiting a much higher stability than the RuO_2 benchmark. From Fig. S12, it can be seen that there is virtually no change in the HER and OER polarization curves at a current density of 10 mA cm^{-2} after 2000 continuous cyclic voltammetry (CV) cycles, suggesting excellent stability in alkaline electrolytes. Moreover, CuRu-CNTs after the long-term stability test were further characterized by TEM image, XRD pattern, Raman spectrum, and high-resolution XPS spectra (Figs. S13, S14), showing no obvious transformation of the carbon support and excellent structural stability. These results confirm the extremely promising longevity of CuRu-CNTs electrocatalysts in the OER, strongly suggesting their potential in practical applications. In summary, the data in Fig. 3i and Table S2 indicate that CuRu-CNTs have the lowest overpotential in both HER and OER processes beyond other synthesized catalysts in this experiment. Additionally, CuRu-CNTs exhibit superior bifunctional performances compared with recently reported catalysts, showing gigantic potential in practical electrochemical applications while reducing the cost of using noble metals (Table S3). Ru with attractive activity and durability is alloyed together with the abundant and inexpensive transition metal Cu as the main dopant. The alloying effect can not only improve the external factors such as site density and charge transfer, but also activate its intrinsic activity [18,64]. CuRu alloy nanoparticles with small particle size and uniform dispersion have modulable electronic properties and a large number of exposed catalytic sites, which enhance the charge transfer and stable catalytic life [29,65,66]. The strong electronic coupling process and the synergic catalysis between Cu and Ru effectively improve the activities of HER and OER.

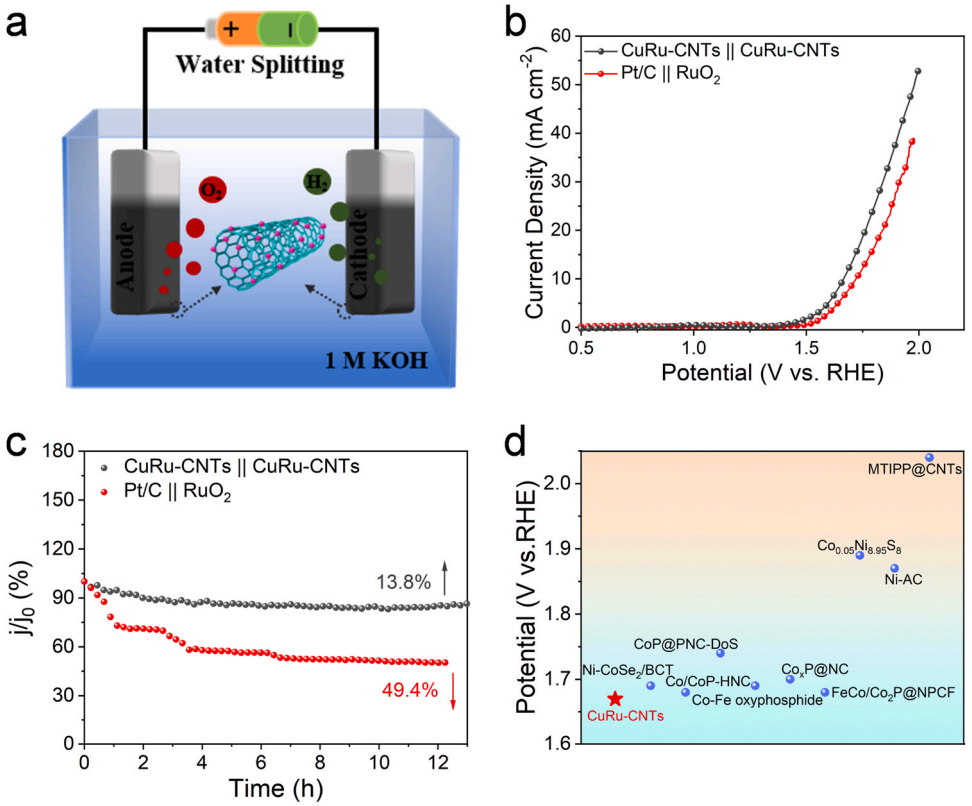

Fig. 4. (a) Schematic of the overall water splitting configuration. (b) Overall water splitting electrocatalysis by the CuRu-CNTs || CuRu-CNTs and the noble benchmark Pt/C || RuO_2. (c) The chronoamperometry test of overall water splitting electrocatalysis (CuRu-CNTs || CuRu-CNTs). (d) Summary of the overall water performance of CuRu-CNTs and other reported electrocatalysts (Table S4).

Based on the experimental results above, we fabricated an alkaline water electrolyzer using CuRu-CNTs as the anode and cathode, respectively (Fig. 4a). Fig. 4b shows the polarization curves of water splitting in 1.0 M KOH solution. At a current density of 10 mA cm^{-2}, the overall water splitting performance of the CuRu-CNTs bifunctional catalyst exhibits superior electrolytic activity compared to the noble metal benchmark Pt/C&RuO_2. Moreover, the electrolyzer is able to maintain a constant current density for more than 12 h with only 13.8 % performance loss (Fig. 4c), showing promising prospects for high-performance overall water splitting in alkaline media. By comparing the results of CuRu-CNTs and some reported metal-based electrocatalysts (Fig. 4d), we discover that the as-obtained CuRu-CNTs material is a promising candidate for catalysts to achieve highly efficient overall water splitting.

The design strategy, which can be extended to other bimetallic or multimetallic alloy nanoparticle catalysts, also provides an alternative approach for catalytic material design in other electrocatalytic applications.

4. Conclusions

In conclusion, a new class of CuRu-CNTs electrocatalysts has been fabricated by a facile wet-chemical strategy followed by an ultrafast flash Joule heating technique. Well-dispersed and ultrasmall CuRu alloy nanoparticles are allowed to uniformly coat the surface of CNTs. The as-synthesized CuRu-CNTs feature both high-performing HER and OER activities in 1 M KOH medium than Pt/C and RuO_2 benchmarks. The catalyst requires low overpotentials, 39 mV for HER and 330 mV for OER, to deliver the current density of 10 mA cm^{-2} (j_{10}). Notably, CuRu-CNTs display excellent stability than commercial Pt/C and RuO_2 under 1.0 M KOH solution over long-term cycle testing. Importantly, the two-electrode electrolyzer assembled by the CuRu-CNTs catalyst for water splitting could offer a low cell voltage to achieve j_{10} and maintained 86.0 % current density over 12 h continuous stability test. The strong binding affinity of alloy nanoparticles and carbon tubes can impede the agglomeration and activity recession of as-developed catalyst. This work offers a facile and ultrafast strategy for alloying, and designing of energy saving and inexpensive catalysts with encouraging performance.

CRediT authorship contribution statement

Wenjie Wei: Investigation, Visualization, Data curation. **Ping Li**: Visualization, Data curation. **Fenghong Lu**: Visualization. **Kaicai Fan**: Visualization. **Bin Li**: Visualization. **Yanze Wei**: Writing – review & editing. **Lingbo Zong**: Conceptualization, Writing – review & editing, Supervision, Funding acquisition.

Data Availability

Data will be made available on request.

Declaration of Competing Interest

The authors declare that they have no known competing financial interests or personal relationships that could have appeared to influence the work reported in this paper.

Acknowledgments

This work was supported financially by the National Natural Science Foundation of China, China (Grant no. 52172208) and the Natural Science Foundation of Shandong Province under Grants ZR2020QB109.

Appendix A. Supporting information

Supplementary data associated with this article can be found in the online version at doi:10.1016/j.jallcom.2022.168349.

References

[1] L. Sun, Q. Luo, Z. Dai, F. Ma, Material libraries for electrocatalytic overall water splitting, Coord. Chem. Rev. 444 (2021) 214049–214085.
[2] Z. Pei, X.F. Lu, H. Zhang, Y. Li, D. Luan, X.W. Lou, Highly efficient electrocatalytic oxygen evolution over atomically dispersed synergistic Ni/Co dual sites, Angew. Chem. Int. Ed. 61 (2022) e202207537–e202207556.
[3] A.H. Al-Naggar, N.M. Shinde, J.-S. Kim, R.S. Mane, Water splitting performance of metal and non-metal-doped transition metal oxide electrocatalysts, Coord. Chem. Rev. 474 (2023) 214864.
[4] B.N. Khiarak, M. Golmohammad, M.M. Shahraki, A. Simchi, Facile synthesis and self-assembling of transition metal phosphide nanosheets to microspheres as a high-performance electrocatalyst for full water splitting, J. Alloy. Compd. 875 (2021) 160049–160060.
[5] C. Huang, P.K. Chu, Recommended practices and benchmarking of foam electrodes in water splitting, Trends Chem. 4 (2022) 1065–1077.
[6] Z. Li, M. Hu, P. Wang, J. Liu, J. Yao, C. Li, Heterojunction catalyst in electrocatalytic water splitting, Coord. Chem. Rev. 439 (2021) 213953–213973.
[7] Z.P. Wu, H. Zhang, S. Zuo, Y. Wang, S.L. Zhang, J. Zhang, S.Q. Zang, X.W. Lou, Manipulating the local coordination and electronic structures for efficient electrocatalytic oxygen evolution, Adv. Mater. 33 (2021) 2103004–2103013.
[8] Y. Luo, Z. Zhang, M. Chhowalla, B. Liu, Recent advances in design of electrocatalysts for high-current-density water splitting, Adv. Mater. 34 (2022) 2108133–2108150.
[9] L. Meng, H. Xuan, X. Liang, Y. Li, J. Yang, P. Han, Flower-like Co_3O_4@NiFe-LDH nanosheets enable high-performance bifunctionality towards both electrocatalytic HER and OER in alkaline solution, J. Alloy. Compd. 919 (2022) 165877–165886.
[10] S. Ravichandran, N. Bhuvanendran, Q. Xu, T. Maiyalagan, L. Xing, H. Su, Ordered mesoporous Pt-Ru-Ir nanostructures as superior bifunctional electrocatalyst for oxygen reduction/oxygen evolution reactions, J. Colloid Interface Sci. 608 (2022) 207–218.
[11] Z. Wang, B. Xiao, Z. Lin, Y. Xu, Y. Lin, F. Meng, Q. Zhang, L. Gu, B. Fang, S. Guo, $PtSe_2$/Pt heterointerface with reduced coordination for boosted hydrogen evolution reaction, Angew. Chem. Int. Ed. 133 (2021) 23576–23581.
[12] P. Yan, Q. Liu, H. Zhang, L. Qiu, H.B. Wu, X.-Y. Yu, Deeply reconstructed hierarchical and defective NiOOH/FeOOH nanoboxes with accelerated kinetics for the oxygen evolution reaction, J. Mater. Chem. A 9 (2021) 15586–15594.
[13] C. Wang, H. Shang, H. Xu, Y. Du, Nanoboxes endow non-noble-metal-based electrocatalysts with high efficiency for overall water splitting, J. Mater. Chem. A 9 (2021) 857–874.
[14] Q. Li, W. Zhang, J. Shen, X. Zhang, Z. Liu, J. Liu, Trimetallic nanoplate arrays of Ni-Fe-Mo sulfide on $FeNi_3$ foam: a highly efficient and bifunctional electrocatalyst for overall water splitting, J. Alloy. Compd. 902 (2022) 163670–163680.
[15] P. Zhang, X.F. Lu, J. Nai, S.Q. Zang, X.W. Lou, Construction of hierarchical Co-Fe oxyphosphide microtubes for electrocatalytic overall water splitting, Adv. Sci. 6 (2019) 1900576–1900582.
[16] A.R. Fareza, F.A.A. Nugroho, F. Abdi, V. Fauzia, Nanoscale metal oxides-2D materials heterostructures for photoelectrochemical water splitting–a review, J. Mater. Chem. A 10 (2022) 8656–8686.
[17] Y. Pei, W. He, M. Wang, J. Wang, T. Sun, L. Hu, J. Zhu, Y. Tan, J. Wang, RuCo alloy trifunctional electrocatalysts with ratio-dependent activity for Zn–air batteries and self-powered water splitting, Chem. Commun. 57 (2021) 1498–1501.
[18] Q. Yao, B. Huang, N. Zhang, M. Sun, Q. Shao, X. Huang, Channel-rich RuCu nanosheets for pH-universal overall water splitting electrocatalysis, Angew. Chem. Int. Ed. 131 (2019) 14121–14126.
[19] B.H. Park, M. Cha, S. Kim, T. Kim, S.W. Joo, O.-S. Jung, M. Kang, Synergistic Ru-Ni-Cu interface for stable hydrogen evolution on 1 % Ru-Ni@Cu alloy grown directly on carbon paper electrode, J. Alloy. Compd. 913 (2022) 165315–165327.
[20] Q. Yang, P. Jin, B. Liu, L. Zhao, J. Cai, Z. Wei, S. Zuo, J. Zhang, L. Feng, Ultrafine carbon encapsulated NiRu alloys as bifunctional electrocatalysts for boosting overall water splitting: morphological and electronic modulation through minor Ru alloying, J. Mater. Chem. A 8 (2020) 9049–9057.
[21] W. Li, Y. Zhao, Y. Liu, M. Sun, G.I. Waterhouse, B. Huang, K. Zhang, T. Zhang, S. Lu, Exploiting Ru-induced lattice strain in CoRu nanoalloys for robust bifunctional hydrogen production, Angew. Chem. Int. Ed. 133 (2021) 3327–3335.
[22] L. Cui, K. Fan, L. Zong, F. Lu, M. Zhou, B. Li, L. Zhang, L. Feng, X. Li, Y. Chen, Sol-gel pore-sealing strategy imparts tailored electronic structure to the atomically dispersed Ru sites for efficient oxygen reduction reaction, Energy Storage Mater. 44 (2022) 469–476.
[23] C. Cai, K. Liu, Y. Zhu, P. Li, Q. Wang, B. Liu, S. Chen, H. Li, L. Zhu, H. Li, Optimizing hydrogen binding on Ru sites with RuCo alloy nanosheets for efficient alkaline hydrogen evolution, Angew. Chem. Int. Ed. 134 (2022) e202113664–e220213669.
[24] T. Lee, Y. Park, H. Kim, Y.K. Hong, E. Hwang, M. Kim, S.K. Kim, D.H. Ha, Restructured Co-Ru alloys via electrodeposition for efficient hydrogen production in proton exchange membrane water electrolyzers, Int. J. Energy Res. 46 (2022) 7975–7987.
[25] S. Zhang, Y. Rui, X. Zhang, R. Sa, F. Zhou, R. Wang, X. Li, Ultrafine cobalt-ruthenium alloy nanoparticles induced by confinement effect for upgrading hydrogen evolution reaction in all-pH range, Chem. Eng. J. 417 (2021) 128047–128053.
[26] Y. Qin, X. Bai, Hydrogenation of N-ethylcarbazole over Ni-Ru alloy nanoparticles loaded on graphitized carbon prepared by carbothermal reduction, Fuel 307 (2022) 121921–121931.
[27] Y. Liu, H. Wen, D. Zhou, X. Huang, X. Wu, J. Jiang, X. Guo, B. Li, Tuning surface d charge of Ni-Ru alloys for unprecedented catalytic activity towards hydrogen generation from ammonia borane hydrolysis, Appl. Catal. B Environ. 291 (2021) 120094–120103.
[28] H. Wang, Y. Yang, F.J. DiSalvo, H.D. Abruña, Multifunctional electrocatalysts: Ru-M (M = Co, Ni, Fe) for alkaline fuel cells and electrolyzers, ACS Catal. 10 (2020) 4608–4616.
[29] X. Huang, Y. Liu, H. Wen, R. Shen, S. Mehdi, X. Wu, E. Liang, X. Guo, B. Li, Ensemble-boosting effect of Ru-Cu alloy on catalytic activity towards hydrogen evolution in ammonia borane hydrolysis, Appl. Catal. B Environ. 287 (2021) 119960–119968.
[30] S. Okazoe, K. Kusada, D. Wu, T. Yamamoto, T. Toriyama, S. Matsumura, S. Kawaguchi, Y. Kubota, H. Kitagawa, Synthesis of Mo and Ru solid-solution alloy NPs and their hydrogen evolution reaction activity, Chem. Commun. 56 (2020) 14475–14478.
[31] T. Kwon, A. Yu, S.-j Kim, M.H. Kim, C. Lee, Y. Lee, Au-Ru alloy nanofibers as a highly stable and active bifunctional electrocatalyst for acidic water splitting, Appl. Surf. Sci. 563 (2021) 150293–150303.
[32] C. Li, L. Zhang, Y. Zhang, Y. Zhou, J. Sun, X. Ouyang, X. Wang, J. Zhu, Y. Fu, PtRu alloy nanoparticles embedded on C_2N nanosheets for efficient hydrogen evolution reaction in both acidic and alkaline solutions, Chem. Eng. J. 428 (2022) 131085–131093.
[33] B. Pang, X. Liu, T. Liu, T. Chen, X. Shen, W. Zhang, S. Wang, T. Liu, D. Liu, T. Ding, Laser-assisted high-performance PtRu alloy for pH-universal hydrogen evolution, Energy Environ. Sci. 15 (2022) 102–108.
[34] M. Zhao, Z. Lyu, M. Xie, Z.D. Hood, Z. Cao, M. Chi, Y. Xia, Pd-Ru alloy nanocages with a face-centered cubic structure and their enhanced activity toward the oxidation of ethylene glycol and glycerol, Small Methods 4 (2020) 1900843–1900850.
[35] K. Ishikawa, J. Ohyama, K. Okubo, K. Murata, A. Satsuma, Enhancement of alkaline hydrogen oxidation reaction of Ru-Ir alloy nanoparticles through bifunctional mechanism on Ru-Ir pair site, ACS Appl. Mater. Interfaces 12 (2020) 22771–22777.
[36] S. Liu, E. Zhang, X. Wan, R. Pan, Y. Li, X. Zhang, M. Su, J. Liu, J. Zhang, Ru-Co-Mn trimetallic alloy nanocatalyst driving bifunctional redox electrocatalysis, Sci. China Mater. 65 (2022) 131–138.
[37] N. Liu, K. Yin, C. Si, T. Kou, Y. Zhang, W. Ma, Z. Zhang, Hierarchically porous nickel-iridium-ruthenium-aluminum alloys with tunable compositions and electrocatalytic activities towards the oxygen/hydrogen evolution reaction in acid electrolyte, J. Mater. Chem. A 8 (2020) 6245–6255.
[38] S. Wang, B. Xu, W. Huo, H. Feng, X. Zhou, F. Fang, Z. Xie, J.K. Shang, J. Jiang, Efficient FeCoNiCuPd thin-film electrocatalyst for alkaline oxygen and hydrogen evolution reactions, Appl. Catal. B Environ. 313 (2022) 121472–121484.
[39] S.-Q. Chang, C.-C. Cheng, P.-Y. Cheng, C.-L. Huang, S.-Y. Lu, Pulse electrodeposited FeCoNiMnW high entropy alloys as efficient and stable bifunctional electrocatalysts for acidic water splitting, Chem. Eng. J. (2022) 137452–137461.
[40] Y. Yang, Y. Yu, J. Li, Q. Chen, Y. Du, P. Rao, R. Li, C. Jia, Z. Kang, P. Deng, Engineering ruthenium-based electrocatalysts for effective hydrogen evolution reaction, Nano-Micro Lett. 13 (2021) 1–20.
[41] D.H. Kweon, M.S. Okyay, S.-J. Kim, J.-P. Jeon, H.-J. Noh, N. Park, J. Mahmood, J.-B. Baek, Ruthenium anchored on carbon nanotube electrocatalyst for hydrogen production with enhanced Faradaic efficiency, Nat. Commun. 11 (2020) 1–10.
[42] Q. Wu, M. Luo, J. Han, W. Peng, Y. Zhao, D. Chen, M. Peng, J. Liu, F.M. De Groot, Y. Tan, Identifying electrocatalytic sites of the nanoporous copper-ruthenium alloy for hydrogen evolution reaction in alkaline electrolyte, ACS Energy Lett. 5 (2019) 192–199.
[43] J. Chen, H. Wang, Y. Gong, Y. Wang, Directly immobilizing a Ru-tannic acid linkage coordination complex on carbon cloth: an efficient and ultrastable catalyst for the hydrogen evolution reaction, J. Mater. Chem. A 7 (2019) 11038–11043.
[44] H. Ejima, J.J. Richardson, K. Liang, J.P. Best, M.P. van Koeverden, G.K. Such, J. Cui, F. Caruso, One-step assembly of coordination complexes for versatile film and particle engineering, Science 341 (2013) 154–157.
[45] B. Lu, L. Guo, F. Wu, Y. Peng, J.E. Lu, T.J. Smart, N. Wang, Y.Z. Finfrock, D. Morris, P. Zhang, Ruthenium atomically dispersed in carbon outperforms platinum toward hydrogen evolution in alkaline media, Nat. Commun. 10 (2019) 1–11.
[46] J. Wei, Y. Liang, Y. Hu, B. Kong, J. Zhang, Q. Gu, Y. Tong, X. Wang, S.P. Jiang, H. Wang, Hydrothermal synthesis of metal-polyphenol coordination crystals and their derived metal/N-doped carbon composites for oxygen electrocatalysis, Angew. Chem. Int. Ed. 128 (2016) 12658–12662.
[47] Y. Wang, S. Chen, S. Zhao, Q. Chen, J. Zhang, Interfacial coordination assembly of tannic acid with metal ions on three-dimensional nickel hydroxide nanowalls for efficient water splitting, J. Mater. Chem. A 8 (2020) 15845–15852.
[48] H. Wang, X. Li, Y. Jiang, M. Li, Q. Xiao, T. Zhao, S. Yang, C. Qi, P. Qiu, J. Yang, A universal single-atom coating strategy based on tannic acid chemistry for multifunctional heterogeneous catalysis, Angew. Chem. Int. Ed. 134 (2022) e202200465–e202200472.
[49] W. Wei, F. Lu, L. Cui, Y. Zhang, Y. Wei, L. Zong, S heteroatom doping in highly porous carbonaceous spheres for boosted oxygen reduction reaction of atomically dispersed Fe-N_4 active sites, Carbon 197 (2022) 112–119.

[50] L. Zong, K. Fan, W. Wu, L. Cui, L. Zhang, B. Johannessen, D. Qi, H. Yin, Y. Wang, P. Liu, Anchoring single copper atoms to microporous carbon spheres as high-performance electrocatalyst for oxygen reduction reaction, Adv. Funct. Mater. 31 (2021) 2104864–2104874.
[51] J. Li, K. Fan, H. Jiang, F. Lu, L. Cui, B. Li, Q. Zhang, G.-C. Fan, L. Zong, L. Wang, Boosting the oxygen reduction reaction behaviour of atomic Fe-N_4 active sites in porous honeycomb-like carbon via P heteroatom doping, J. Mater. Chem. A 10 (2022) 18147–18155.
[52] F. Lu, K. Fan, L. Cui, Y. Yang, W. Wang, G. Zhang, C. Wang, Q. Zhang, B. Li, L. Zong, Cu-N_4 single atoms derived from metal-organic frameworks with trapped nitrogen-rich molecules and their use as efficient electrocatalysts for oxygen reduction reaction, Chem. Eng. J. 431 (2022) 133242.
[53] W. Zhang, L. Zong, K. Fan, L. Cui, Q. Zhang, J. Zhao, L. Wang, S. Feng, Enabling highly efficient electrocatalytic oxygen reduction and evolution reaction by established strong MnO/Co-support interaction, J. Alloy. Compd. 874 (2021) 159965-15997.
[54] X. Liu, S. Xi, H. Kim, A. Kumar, J. Lee, J. Wang, N.Q. Tran, T. Yang, X. Shao, M. Liang, Restructuring highly electron-deficient metal-metal oxides for boosting stability in acidic oxygen evolution reaction, Nat. Commun. 12 (2021) 1–11.
[55] B. Li, Z. Li, Q. Pang, J.Z. Zhang, Core/shell cable-like Ni_3S_2 nanowires/N-doped graphene-like carbon layers as composite electrocatalyst for overall electrocatalytic water splitting, Chem. Eng. J. 401 (2020) 126045–126073.
[56] K. Qu, Y. Zheng, S. Dai, S.Z. Qiao, Polydopamine-graphene oxide derived mesoporous carbon nanosheets for enhanced oxygen reduction, Nanoscale 7 (2015) 12598–12605.
[57] X. Du, S. Luo, H. Du, M. Tang, X. Huang, P.K. Shen, Monodisperse and self-assembled Pt-Cu nanoparticles as an efficient electrocatalyst for the methanol oxidation reaction, J. Mater. Chem. A 4 (2016) 1579–1585.
[58] S. Bai, Q. Yao, Y. Xu, K. Cao, X. Huang, Strong synergy in a lichen-like RuCu nanosheet boosts the direct methane oxidation to methanol, Nano Energy 71 (2020) 104566–104574.
[59] Q. Feng, Q. Wang, Z. Zhang, Y. Xiong, H. Li, Y. Yao, X.-Z. Yuan, M.C. Williams, M. Gu, H. Chen, Highly active and stable ruthenate pyrochlore for enhanced oxygen evolution reaction in acidic medium electrolysis, Appl. Catal. B Environ. 244 (2019) 494–501.
[60] Z.L. Zhao, Q. Wang, X. Huang, Q. Feng, S. Gu, Z. Zhang, H. Xu, L. Zeng, M. Gu, H. Li, Boosting the oxygen evolution reaction using defect-rich ultra-thin ruthenium oxide nanosheets in acidic media, Energy Environ. Sci. 13 (2020) 5143–5151.
[61] K. Yang, P. Xu, Z. Lin, Y. Yang, P. Jiang, C. Wang, S. Liu, S. Gong, L. Hu, Q. Chen, Ultrasmall Ru/Cu-doped RuO_2 complex embedded in amorphous carbon skeleton as highly active bifunctional electrocatalysts for overall water splitting, Small 14 (2018) 1803009–1803018.
[62] H. Zhang, W. Zhou, J. Dong, X.F. Lu, X.W.D. Lou, Intramolecular electronic coupling in porous iron cobalt (oxy)phosphide nanoboxes enhances the electrocatalytic activity for oxygen evolution, Energy Environ. Sci. 12 (2019) 3348–3355.
[63] J. Liu, Z. Wang, X. Wu, D. Zhang, Y. Zhang, J. Xiong, Z. Wu, J. Lai, L. Wang, Pt doping and strong metal-support interaction as a strategy for NiMo-based electrocatalysts to boost the hydrogen evolution reaction in alkaline solution, J. Mater. Chem. A 10 (2022) 15395–15401.
[64] J. Zhao, T. Pan, J. Sun, H. Gao, J. Guo, Cu-Ru nanoalloys on carbon black for efficient production of hydrogen in neutral and alkaline conditions, Mater. Lett. 262 (2020) 127041.
[65] Z. Cui, S. Duan, S. Yao, T. Pan, D. Dai, H. Gao, Investigation of the electrocatalytic activity of CuRu alloy and its mechanism for hydrogen evolution reaction, ChemElectroChem 8 (2021) 705–711.
[66] H. Huang, H. Jung, S. Li, S. Kim, J.W. Han, J. Lee, Activation of inert copper for significantly enhanced hydrogen evolution behaviors by trace ruthenium doping, Nano Energy 92 (2022) 106763.